Chemical Treatment of PLA Composite Waste for Resource Recovery

Eva Domincova Bergerova[1*], Jaroslav Cisar[1], Monika Strasakova[1], Simona Uhercova[1], Dominika Hanusova[1], Miroslava Dusankova[1], David Skoda[1], Vladimir Sedlarik[1]

[1]Centre of Polymer Systems, University Institute, Tomas Bata University in Zlin, tr. Tomase Bati 5678,760 01 Zlin, Czech Republic

*Corresponding author: Eva Domincova Bergerova, domincova_bergerova@utb.cz

Abstract

The increasing use of PLA (polylactic acid) materials has led to growing amounts of composite waste containing industrial additives that complicate end-of-life treatment. Although alcoholysis represents a promising chemical treatment route for the depolymerization of PLA and recovery of value-added products, systematic studies addressing commercially relevant PLA composites under comparable alcoholysis conditions remain scarce. This study investigates the alcoholysis depolymerization of PLA-based composites containing typical industrial components, including calcium carbonate (1–10 wt%), carbon black, plasticizers, cellulose, and minor polymeric components. Depolymerization was performed in an acetone/ethanol system at 70 °C using the organocatalyst 1,5,7-triazabicyclo[4.4.0]dec-5-ene, enabling recovery of ethyl lactate, a bio-based solvent.

Depolymerization efficiencies ranged from 61–100%, depending on composite composition and material structure. High depolymerization efficiencies and PLA conversion to ethyl lactate were obtained for materials with low additive content. PLA conversion reached up to 98% for neat PLA. Higher inorganic filler content (>2%) and cellulose-rich composites showed markedly reduced depolymerization and product formation. Structural and thermal

characterization demonstrated differences in crystallinity, thermal stability, and accessibility of the PLA phase, thereby affecting alcoholysis performance. This work provides practical insight into the chemical treatment of PLA composite waste under mild conditions and highlights the potential for resource recovery through ethyl lactate production.

Keywords: poly(lactic acid); PLA composite waste; chemical treatment; alcoholysis; resource recovery

1. Introduction

The increasing demand for sustainable polymeric materials has led to the widespread use of poly(lactic acid) (PLA), particularly in packaging, agriculture, and technical applications (Ghanbarzadeh and Almasi, 2013; Künkel et al., 2016; Samir et al., 2022). In industrial practice, PLA is rarely used as a neat polymer and is typically formulated as composite materials containing mineral fillers, plasticizers, pigments, fibers, or secondary polymers to improve mechanical performance, thermal stability, and processability (Alaerts et al., 2018; Aliotta et al., 2017; Balla et al., 2021; Behrens, 2016; Carné Sánchez and Collinson, 2011; González-López et al., 2020; Liu et al., 2010; Quiles-Carrillo et al., 2018; Schneider et al., 2020; Shorey and Mekonnen, 2024; Siddiqui et al., 2021; Spinelli et al., 2018; Szatkowski et al., 2024; Thumsorn et al., 2022; Zdanowicz et al., 2024). As a result, most commercially available PLA products and post-consumer waste streams consist of multi-component, additive-containing materials rather than virgin PLA.

The production of PLA is associated with a cumulative energy demand of approximately 50–60 GJ t^{-1} (14–17 MWh t^{-1}), depending on the production route and system boundaries. When additional processing steps such as melt extrusion into filaments or films are included, the

total energy demand for finished PLA products can reach 54–79 GJ t^{-1} (15–22 MWh t^{-1}) (Erwin et al, 2015; Erwin et al, 2003). This embedded energy is irreversibly lost during biodegradation of PLA (Auras et al., 2004; Erwin et al., 2015; Erwin et al, 2003). In contrast, solvolysis enables recovery of ethyl lactate, whose conventional synthesis from lactic acid requires more than 30–40 GJ t^{-1} (8–11 MWh t^{-1}) (Rathin Datta, 2006), highlighting the potential energy advantage of chemical recycling over both composting and virgin solvent production.

Mechanical recycling of PLA composites is technologically simple but suffers from significant drawbacks, including chain scission, molecular weight reduction, deterioration of mechanical properties, and poor dispersion of fillers upon repeated processing, resulting in limited recyclate quality and low recycling rates (Arrigo et al., 2020; Betancourt and Cree, 2017; Finnerty et al., 2023; González-López et al., 2020; Pudełko et al., 2021; Xia et al., 2024). Composting is often presented as an end-of-life option for PLA composites; however, its applicability is particularly limited for multi-component materials, where the presence of additives complicates processing and reduces overall recycling efficiency. Moreover, composting leads to irreversible loss of the material value and embedded energy, as the polymer is converted into CO_2, water, and biomass (Geyer et al., 2017; Pavon et al., 2022; Thakur et al., 2018; Tonini et al., 2021; Yadav et al., 2021).

Accordingly, chemical treatment has emerged as a more controllable and resource-efficient strategy for managing PLA waste within a circular economy framework. Depolymerization enables conversion of PLA into value-added products such as ethyl lactate, a bio-based solvent with low toxicity, biodegradability, and favourable solvency properties (Leibfarth et al., 2012; Majgaonkar et al., 2021; Siddiqui et al., 2021). However, the practical feasibility of

chemical recycling critically depends on its performance in additive-containing PLA waste streams, which dominate post-consumer PLA waste.

Selective chemical treatment through alcoholysis has therefore attracted increasing attention as a promising approach for recovering high-value products (Azarian and Sutapun, 2022; Leibfarth et al., 2012; Liendo et al., 2022; Majgaonkar et al., 2021). Solvolysis enables depolymerization under relatively mild conditions with high product purity and is therefore considered a suitable approach for the recycling of PLA composite materials (des Ligneris et al., 2020; Ellis et al., 2024; Román-Ramírez et al., 2020). Nevertheless, most published studies focus on neat PLA or simplified laboratory systems. Systematic investigations addressing industrially relevant, additive-rich PLA composites under comparable reaction conditions remain scarce, representing a critical knowledge gap.

In our previous work (Bergerova et al., 2025), we demonstrated that the solvolysis depolymerization of virgin PLA is strongly governed by polymer architecture and crystallinity. However, such virgin PLA systems do not reflect the complexity of additive-containing PLA materials, where multiple components and heterogeneous structures may significantly influence degradation behaviour. Such multi-component materials dominate industrial applications and post-consumer waste streams. Therefore, this study addresses a critical knowledge gap by investigating PLA composites representative of real industrial practice. Specifically, composites containing calcium carbonate, carbon black, plasticizers, cellulose, and secondary polymers were selected, as these additives are widely used in commercial PLA products to tailor cost, stiffness, thermal behaviour, coloration, and processability (Alaerts et al., 2018; Aliotta et al., 2017; Behrens, 2016; Carné Sánchez and Collinson, 2011; González-López et al., 2020; Liu et al., 2010; Quiles-Carrillo et al., 2018; Schneider et al., 2020; Shorey and Mekonnen, 2024; Siddiqui et al., 2021; Spinelli et al.,

2018; Szatkowski et al., 2024; Thumsorn et al., 2022; Zdanowicz et al., 2024). The selected materials were intended to represent commercially relevant PLA-based products containing common classes of industrial additives, including mineral fillers, pigments, plasticizers, biodegradable copolymers, and natural fibres. To date, a systematic evaluation of how such additive-rich PLA composites behave under comparable and well-controlled reaction conditions has not been comprehensively reported in the literature. Recent studies have demonstrated the growing diversity of PLA-based hybrid composites incorporating inorganic and waste-derived fillers, including recycled materials reinforced with metallic particles and composites containing bio-derived fillers (Coman et al., 2026; Tadi and Mamilla, 2025). These developments highlight the increasing compositional complexity of PLA-based materials and the need for suitable end-of-life strategies for heterogeneous PLA composite waste. Rather than investigating the isolated effect of individual additives in simplified model systems, the present work evaluates the behaviour of representative PLA composite materials in their original industrial form under chemical treatment conditions.

The aim of this work is to evaluate the behaviour of commercially relevant PLA composites during chemical treatment under mild alcoholysis conditions and to investigate the formation of ethyl lactate as a value-added product. Particular attention was devoted to evaluating how differences in composition and material structure affect depolymerization behaviour and ethyl lactate formation in commercially relevant PLA composites. Alcoholysis was performed in an acetone/ethanol system using an organocatalyst under comparable reaction conditions. By combining depolymerization experiments with structural and thermal characterization, the behaviour of PLA composite materials during depolymerization was evaluated.

The key innovative contribution of this study lies in extending alcoholysis from virgin PLA to industrially relevant multi-component PLA materials in their original form, enabling the

influence of material composition and structure on depolymerization behaviour and ethyl lactate formation to be assessed under practically relevant conditions.

2. Materials and methods

2.1 Materials

Chemicals (acetone, ethanol, ethyl lactate standards, and 1,5,7-triazabicyclo[4.4.0]dec-5-ene (TBD catalyst) were purchased from commercial suppliers and used as received, in accordance with the procedure described in our previous work (Bergerova et al., 2025). Virgin PLA (Ingeo 2003D, PLA-A; weight-average molecular weight (M_w): 150—200 kDa ± 4000 Da, polydispersity index (PDI): 1.7—1.8) was used as a reference material for evaluating depolymerization efficiency and ethyl lactate formation (Table 1). The PLA samples denoted B and C were prepared by the authors' team (Cisar et al., 2023). PLA samples D–E were obtained from the specified sources; however, the manufacturer does not disclose the exact composition of the material. Therefore, the amount of additives was evaluated based on analyses conducted in our laboratory. The additive content was estimated using a complementary thermogravimetric analysis (TGA), differential scanning calorimetry (DSC), and Fourier transform infrared spectroscopy (FTIR) analyses, while X-ray fluorescence (XRF) measurements were used to verify the elemental composition of selected samples as described in Sections 2.3.3–2.3.6. The obtained values should therefore be considered approximate and were used primarily for material classification and comparison purposes. Data on all tested materials, including their composition and producer, are given in Table 1.

Table 1 Overview of the tested PLA materials (original form), their composition and supplier

Sample	specification	sample composition	supplier
PLA-A	PLA granules	PLA Ingeo™ 2003D	NatureWorks®
PLA-B	PLA filaments	PLA + 1% $CaCO_3$ + 0.5% CA	NatureWorks®/ own preparation
PLA-C	PLA foil	PLA + 10% $CaCO_3$ +4% plasticizer*	NatureWorks®/ own preparation
PLA-D	PLA woven stack	PLA + 1.5% $CaCO_3$ + (<1%) DETPE	Czech Fibre, CZ
PLA-E	PLA sackcloth	PLA + 1% $CaCO_3$ + (<1%) PBAT + 0.5% CA	Juta, CZ
PLA-F	PLA laminate	PLA + 3.5% $CaCO_3$ + (>50%) cellulose	Oxalis, CZ

* plasticizer (copolymer PLA/PEG) – (Cisar et al., 2023)

CA – carbon black

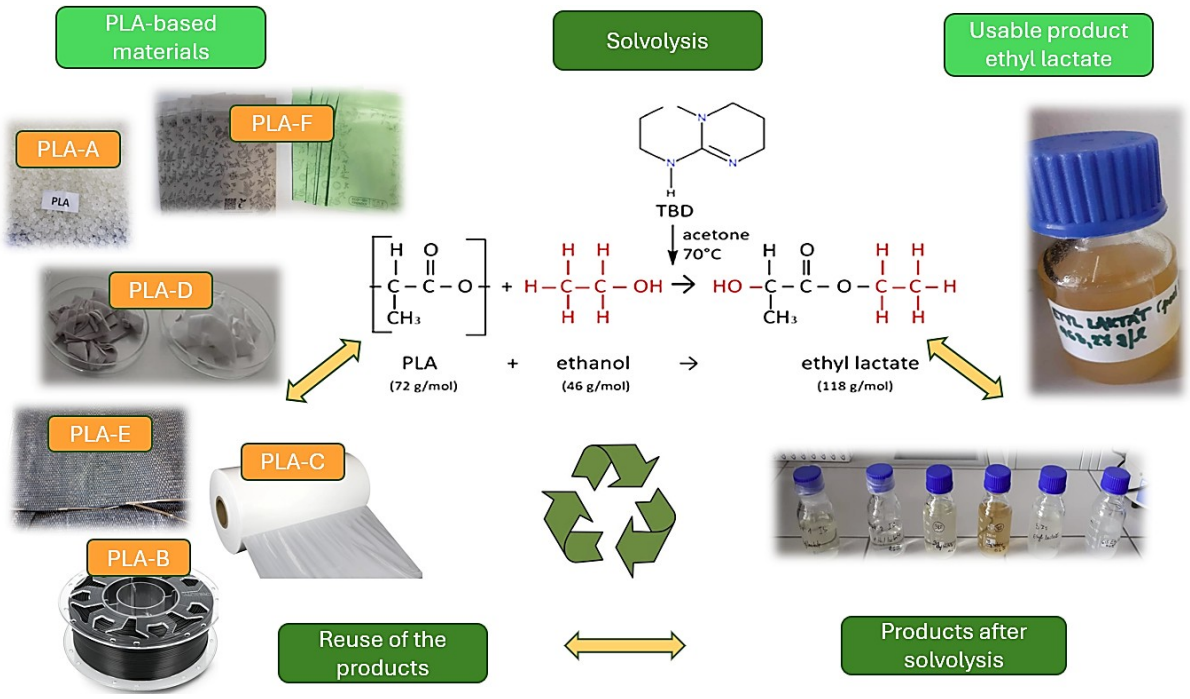
DETPE – diethyl-p-phthalate, PBAT - polybutylene adipate terephthalate

Based on their original material forms, the investigated PLA-based materials may be relevant to applications in filament-based products, films, and foils, woven and textile materials, sackcloth products, and laminated structures.

2.2 Experimental strategy

The experimental procedure was based on our previous work (Bergerova et al., 2025), with modifications as described below. The reaction conditions (acetone as solvent, ethanol as nucleophile, and TBD as catalyst at 70 °C) were kept consistent to enable direct comparison between the degradation behaviour of virgin PLA reported earlier and the additive-rich composites studied here. The reaction temperature of 70 °C was selected based on our previous optimization study, in which this temperature provided the most effective PLA depolymerization under the selected acetone/ethanol/TBD reaction conditions (Bergerova et al., 2025). The composition of the tested PLA materials differed, as detailed in Table 1. The depolymerization procedure was carried out under mild reaction conditions (Scheme 1). Following the alcoholysis reaction, the liquid fraction was concentrated under reduced pressure using a vacuum evaporator to remove residual volatile solvents, predominantly

ethanol and acetone, and to obtain an ethyl lactate-enriched product fraction. The depolymerization proceeds via alcoholysis of ester bonds, as reported in the literature (Leibfarth et al., 2012; Majgaonkar et al., 2021).



Scheme 1 Alcoholysis as a type of solvolysis of PLA-based composite materials to ethyl lactate under mild reaction conditions

The reaction mixture was maintained at 70 °C for periods of 30 to 120 minutes, depending on the sample form, after which the reaction mixture was filtered into an Erlenmeyer flask. Filtration was performed using a glass filter funnel (10 cm) equipped with KA 5-M filter paper (Perštejn, Czech Republic), with a particle retention of 3 µm.

Experiments were conducted using a solid loading of 14.3 wt% for the denser PLA-A and PLA-B materials and 4.04 wt% for the lighter PLA-C–PLA-F materials. The lower mass used for the latter samples was dictated by their significantly lower bulk density and substantially larger occupied volume. Although the solvent-to-nucleophile ratio and catalyst loading relative to the PLA content were maintained consistently, the different solid loadings represent

an experimental limitation when directly comparing the absolute conversion and kinetic parameters between PLA-A/B and PLA-C–F. Therefore, the cross-comparison of these materials is interpreted primarily in terms of overall trends in their alcoholysis behaviour rather than as a strictly quantitative comparison of intrinsic reaction kinetics. Preliminary experiments showed that loading larger quantities of these fibrous, textile-based, or laminated materials would exceed the effective working volume of the reactor and impair efficient mixing, resulting in poor contact between the polymer matrix, solvent, nucleophile, and catalyst. Therefore, the feed mass was adjusted according to the physical volume of the investigated materials while maintaining identical solvent-to-nucleophile ratios and catalyst loading relative to the PLA content. This approach enabled the different material forms to be processed while maintaining efficient mass transfer within the reaction system. The samples were prepared using a solvent-to-nucleophile ratio of 1:2 and a catalyst amount of 2 wt% relative to the PLA mass. TBD, a bicyclic guanidine catalyst, was used as described in our previous work (Bergerova et al., 2025).

The overall degree of material decomposition was determined gravimetrically from the initial sample mass and the mass of the dry solid residue recovered after filtration according to Equation (*1*). The solid residue was not separated into individual PLA and non-PLA components and therefore included unreacted PLA, where present, together with insoluble or non-converted components such as $CaCO_3$, carbon black, and cellulose. Accordingly, this parameter represents the overall gravimetric decomposition of the PLA-based material rather than the selective degradation of the PLA fraction. In addition, the conversion of PLA to ethyl lactate (EL) was calculated based on the amount of EL formed, assuming a one-to-one stoichiometry between the PLA repeating unit and ethyl lactate, as described by Equation (*2*) (Bergerova et al., 2025). Additives such as carbon black and $CaCO_3$ remained on the filter together with the unreacted polymer matrix, while plasticizer passed into the filtrate.

The overall degree of material decomposition $D_{(M)}$ was determined by Equation (*1*):

$$D_{(M)} = \frac{w_0 - w_1}{w_0} x\, 100\,\% \qquad (1)$$

where w_0 represents the initial mass of PLA-based material and w_1 represents the mass of the dry solid residue recovered after alcoholysis and filtration.

The conversion of the PLA fraction to EL, *X*(PLA), was calculated according to Equation (2):

$$X_{(PLA)} = \frac{w_3}{w_0} x \frac{M(PLA)}{M(EL)} x\, 100\,\% \qquad (2)$$

where w_0 represents the initial amount of PLA, w_3 represents the mass of the ethyl lactate obtained, and $M_{(PLA)}$ = 72.06 g·mol^{-1} and $M_{(EL)}$ = 118.13 g·mol^{-1} are the molar masses of the PLA repeating unit and ethyl lactate, respectively.

It should be noted that $X_{(PLA)}$ was calculated based on the amount of ethyl lactate formed and therefore does not necessarily correspond to the gravimetrically determined $D_{(M)}$.

2.3 Characterization of the end product and determination of PLA decomposition

2.3.1 GC-FID

Gas chromatography with flame ionization detection (GC-FID) was performed using a Shimadzu GC 2010 Plus gas chromatograph (Shimadzu, Kyoto, Japan) and was used to determine ethyl lactate concentration and to quantify residual ethanol, acetone, and lactide. The analysis was performed using the previously optimized protocol described in (Bergerova et al., 2025). Samples were filtered (0.22 µm) of polytetrafluoroethylene (PTFE) and diluted 10-fold in methanol prior to analysis. Quantification of ethyl lactate, ethanol, acetone, and

lactide was carried out using calibration curves (R^2 = 0.999). Helium served as carrier gas, and all measurements were performed in triplicate.

2.3.2 GPC

Gel permeation chromatography (GPC) was performed using a Waters HPLC system equipped with Water differential reactometers e2695 and 2414 (Waters Corporation, USA) and employed to characterize molecular weight distribution and polydispersity of PLA before and after degradation, as well as polymer residues in the reaction mixture. The analysis was performed under conditions identical to those described in our previous work (Bergerova et al., 2025). Samples were dissolved in THF, filtered (0.45 µm PTFE), and, when necessary, treated with ultrasound to ensure complete dissolution. All data were processed in Empower 3 software.

2.3.3 FTIR

Attenuated total reflectance Fourier transform infrared spectroscopy (ATR-FTIR) was performed using a Nicolet iS5 spectrometer equipped with a germanium crystal (Thermo Fisher Scientific, Waltham, USA) and used to analyze structural changes in PLA before and after degradation, as well as in the ethyl lactate product. The measurements were performed according to the procedure established in our earlier study (Bergerova et al., 2025).

2.3.4 Thermal analysis (DSC and TGA)

Differential scanning calorimetry (DSC) was performed using a DSC1 STAR system (Mettler Toledo, Switzerland), while thermogravimetric analysis (TGA) was carried out using a TAQ500 thermogravimetric analyser (V20.13, Build 39). DSC and TGA were used to assess thermal properties and structural changes of PLA materials before and after degradation. The measurements were performed under conditions identical to those described in our previous work (Bergerova et al., 2025). The glass transition temperature (T_g),

crystallization behaviour, and melting temperature (T_m) were evaluated from DSC thermograms, while TGA was used to assess thermal stability. The degree of crystallinity (χc) was calculated according to Equation (3), where ΔH^0_m is the heat of fusion of 100% crystalline PLA (93.1 $J \cdot g^{-1}$). Thermogravimetric analysis (TGA) samples were prepared in accordance with previously reported procedures (Cvek et al., 2022; Ineke Velghe, MURA-KAMI, 1993; Velghe et al., 2023). For thermal analyses, all samples, whether granules, filaments, films, woven stack, laminate, or sackcloth, were cut into slices to ensure that the sample compactly covered the bottom of the crucible. This guaranteed the planarity and parallel orientation of the sample during measurement, enabling efficient heat transfer.

The degree of crystallinity χ_c (%) was calculated according to Equation 3 below:

$$\chi c = \frac{\Delta H_m - \Delta H_c}{\Delta H^0_m} x\, 100\,\% \qquad (3)$$

where ΔH_m is the heat of fusion, ΔH_c represents cold-crystallization enthalpy ($J \cdot g^{-1}$) and ΔH^0_m is the tabulated heat of fusion for the theoretically 100% crystalline PLA homopolymer (93.1 $J \cdot g^{-1}$) (Leibfarth et al., 2012; Signori et al., 2009).

2.3.5 X-ray diffraction

X-ray diffraction (XRD) measurements were performed using a Rigaku MiniFlex 600 diffractometer equipped with a CoKα X-ray tube. XRD analysis of PLA samples was using the previously optimized protocol described in (Bergerova et al., 2025). For selected samples (PLA-B and PLA-F), approximately 1 g of material was dissolved in chloroform and deposited onto the sample holder. Diffractograms were recorded after solvent evaporation.

2.3.6 Elemental analysis

Energy-dispersive X-ray fluorescence (EDX-XRF) analysis was performed using an ARL Quant'EDX-RF analyser (Thermo Fisher Scientific). Elemental analysis by EDX-XRF was performed to verify the absence of metallic and mineral elements in the ethyl lactate products. The measurements were carried out under conditions identical to those described in our previous work (Bergerova et al., 2025). Samples were analyzed directly without dilution.

2.3.7 Statistical analysis

Every measurement was taken a minimum of three times in this study. The reported relative standard deviations (RSD) values represent the relative standard deviation calculated from at least three measurements, providing an estimate of experimental variability, as reflected in error bars or table values. Statistical comparisons were provided by one-way analysis of variance (ANOVA), and differences were considered significant at $P < 0.05$, OriginPro 2024 SR1 (OriginLab Corporation, USA).

2.3.8 Evaluation of degradation kinetics

The degradation kinetics were analyzed using an integrated pseudo-first-order rate equation *(4):*

$$\ln(1-X) = -k \cdot t \quad (4)$$

where X represents the conversion of PLA, t denotes the reaction time, and k corresponds to the apparent pseudo-first-order rate constant. The apparent rate constant k was calculated according to Equation *(5)*:

$$k = \frac{-\ln(1-X)}{t} \quad (5)$$

3. Results and Discussion

3.1 Chemical treatment of PLA composite waste and its conversion to EL

The depolymerization behaviour of PLA composites differed significantly from that previously observed for virgin PLA (Bergerova et al., 2025; Leibfarth et al., 2012; Majgaonkar et al., 2021), particularly with respect to additive content and material structure. A representative set of PLA composite materials, including composite waste (PLA-B, PLA-F) and the pure PLA granulate (PLA-A) was therefore selected for comparative evaluation (Table 1). Under the applied reaction conditions, pronounced differences in degradation efficiency and ethyl lactate formation were observed among the investigated materials (Table 2, Figure 1). $X_{(PLA)}$ – conversion of the PLA fraction in the composite material to ethyl lactate; for composite samples, the initial PLA amount was calculated by subtracting the known or estimated content of non-PLA components from the initial sample mass.

Table 2 Reaction parameters of alcoholysis and data on sample and product decomposition

Conditions: 70 °C; 2 wt% TBD; ratio of 1: 2 solution-nucleophile (acetone - ethanol) in a 500- mL reaction flask

Sample	**specification**	**input amount (g)**	**$D_{(M)}$ (%)**	**time (min)**	**c ($g \cdot L^{-1}$)[a]**	**c ($g \cdot L^{-1}$)[b]**	**$X_{(PLA)}$ (%)**
PLA-A	granules	40	100.00	120	362.00	968.00	98.80
PLA-B	filaments	40	95.00	120	268.52	631.40	69.18
PLA-C	foil	10	68.75	60	227.40	307.40	32.06
PLA-D	woven stack	10	100.00	30	80.87	884.11	87.43
PLA-E	sackcloth	10	93.00	120	38.37	797.32	87.44
PLA-F	laminate	10	61.00	120	3.82	24.64	100.00*

c ($g \cdot L^{-1}$)[a] - concentration of the ethyl lactate product following the reaction and prior to cleaning

c ($g \cdot L^{-1}$)[b] - [the] concentration of the ethyl lactate product after cleaning using vacuum evaporator

$X_{(PLA)}$ – conversion of the PLA fraction to ethyl lactate; for composite materials, the initial PLA amount used for the calculation was corrected by subtracting the known or estimated content of non-PLA components from the initial sample mass

* For PLA-F, *X*(PLA) represents an approximate conversion of the PLA fraction because the exact PLA/cellulose ratio in this commercial laminate was not disclosed by the manufacturer; the material contains >50 wt% cellulose.

RSD of concentration measurements: 4.8 ± 0.4% (three or more measurements, no statistically significant differences were observed between replicate measurements, $P > 0.05$)

The overall degree of material decomposition was strongly dependent on material composition. Complete material decomposition (100%) was observed solely in specimens of the pure polymer (PLA-A) and PLA-based woven stack (PLA-D), both with a high proportion of polylactic acid (≥ 98 wt%). The PLA filament (PLA-B) and sackcloth (PLA-E) samples also exhibited a high degree of material decomposition, as their PLA content remained high (> 90 wt%), although they also contained admixtures of additives which could not be removed by the alcoholysis reaction (ca 5-7 wt%). The PLA film (PLA-C) and laminate (PLA-F) exhibited material decomposition below 70%. This behaviour may be associated with their higher content of non-PLA components, including cellulose in PLA-F and inorganic filler (>2%) in PLA-C; however, differences in material form, PLA grade, molecular characteristics, crystallinity, and structure may also contribute to the observed degradation behaviour. The degree of decomposition was compared with the conversion of PLA to ethyl lactate, the main product of solvolysis (Table 2, Figure 1). For PLA-F, the reported *X*(PLA) value should be regarded as approximate because the exact PLA/cellulose ratio in this commercial laminate was not disclosed by the manufacturer. The overall material decomposition was evaluated by comparing the initial sample mass with the recovered solid residue after filtration, confirming that incomplete depolymerization corresponded to the presence of non-converted components, particularly inorganic fillers such as $CaCO_3$ and carbon black. The higher the degree of decomposition, the greater the conversion of PLA to ethyl lactate, reflecting the higher accessibility of reactive ester bonds within the PLA matrix,

in agreement with our previous findings on PLA alcoholysis (Bergerova et al., 2025). To concentrate the ethyl lactate-containing product, the volatile solvent fraction, predominantly ethanol and acetone, was removed under reduced pressure using a vacuum evaporator (Table 2). The evaporation conditions had been optimized in previous experiments to minimize co-evaporation of ethyl lactate. Therefore, significant EL losses were not expected, although minor losses during solvent removal cannot be completely excluded.

For samples that did not undergo complete alcoholysis depolymerization, the remaining solid fraction was separated by filtration after completion of the reaction. This solid residue consisted predominantly of components originally present in the composite materials that were not susceptible to solvolysis, including cellulose fibers, inorganic fillers (e.g., $CaCO_3$), carbon black, and minor fractions of secondary polymers. These residual solid fractions represent potentially valuable secondary materials, which could be further utilized as cellulose-rich fillers, inorganic additives, or carbon-based materials, rather than being discarded as waste. The recovery of this fraction reflects the partial decomposition of the PLA matrix in these materials and the persistence of constituents that were not completely solvolytically converted under the applied conditions, particularly $CaCO_3$, carbon black, and more resistant cellulose-rich fractions. Nevertheless, depending on its dispersion and interfacial interactions with the PLA matrix, carbon black may locally affect polymer-chain mobility and accessibility of the PLA phase through filler aggregation or network formation, potentially influencing the heterogeneous alcoholysis behaviour (Tsou et al., 2025).

Sample PLA-E contained a minor amount of PBAT (<1 wt%), which may also undergo partial degradation under alcoholysis conditions due to the presence of ester bonds in its structure. However, considering its low concentration in the composite and the absence of significant additional chromatographic peaks, attribution of PBAT-derived products to the final product stream is expected to be limited. No significant additional chromatographic peaks attributable

to PBAT degradation products were observed under the applied analytical conditions. Similarly, possible structural changes in other organic components present in the investigated composites cannot be excluded under the applied alcoholysis conditions. Ester-containing components, including DETPE and the PLA/PEG-based plasticizer, may potentially undergo partial alcoholysis or transesterification in the ethanol/TBD reaction medium. In the cellulose-rich material, interactions with the reaction medium, including swelling or surface modification of cellulose, may also occur. These potential changes were not directly investigated in the present study, which focused on PLA conversion to ethyl lactate, and their detailed characterization would require targeted analysis of the individual organic components and their reaction products.

The extent of material decomposition $D_{(M)}$ does not always correspond directly to the conversion to ethyl lactate $X_{(PLA)}$, as additives in the original material can reduce product formation even when the polymer matrix is substantially decomposed (Bergerova et al., 2025; Leibfarth et al., 2012). These additives can impair product quality and, even after purification, may lead to a decreased amount of the final product (e.g. PLA-B; Figure 1, Table 2).

In addition, a fraction of the degraded PLA may remain in the reaction mixture as soluble oligomeric species or intermediate degradation products that are not fully converted to ethyl lactate under the applied conditions. Therefore, the gravimetrically determined material decomposition degree $D_{(M)}$ may exceed the experimentally determined conversion to ethyl lactate X(PLA).

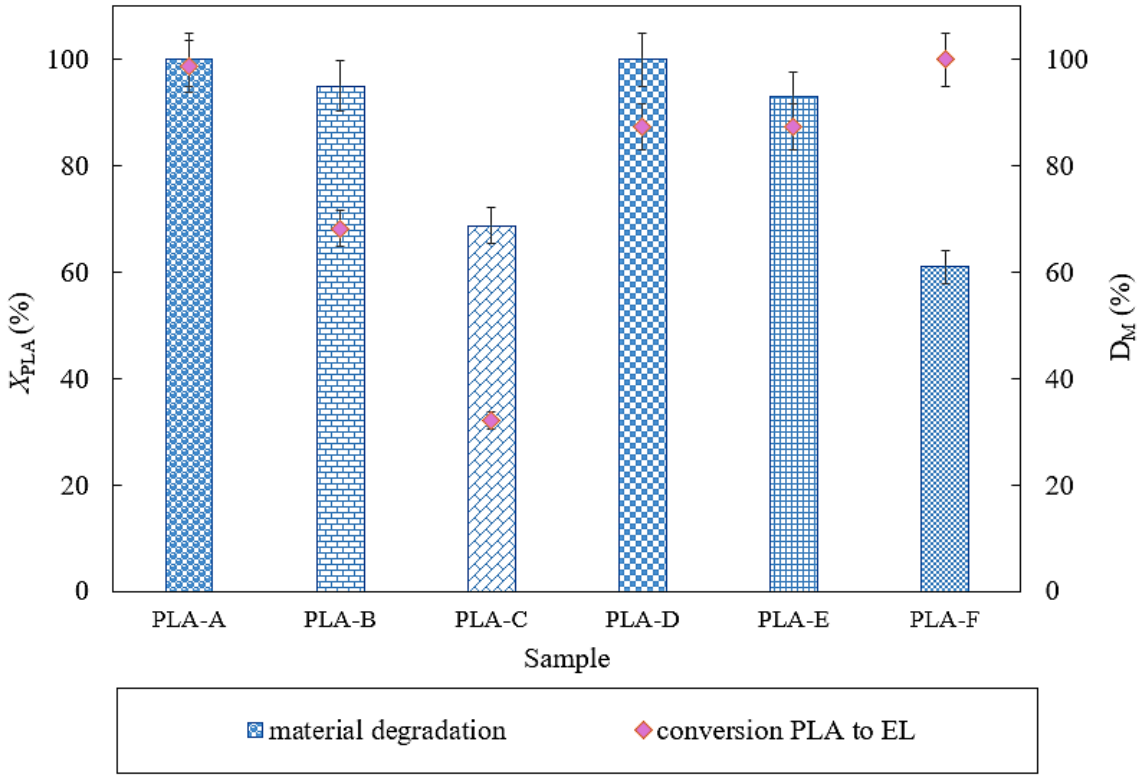


Figure 1 Effect of alcoholysis on mixed PLA materials (A–F), showing overall material decomposition and PLA conversion to ethyl lactate. RSD: 5.0 ± 0.5% for material decomposition and 2.1 ± 0.3% for polymer conversion (at least three measurements); no statistically significant differences were observed between replicate measurements ($P > 0.05$).

The course of PLA conversion for the individual samples, in relation to ethyl lactate, is shown in Figure 2. PLA-A showed a slower increase in polymer conversion during the first 120 minutes compared to PLA-B, PLA-C, and PLA-D. For PLA-A, once complete decomposition had occurred, a concentrated ethyl lactate-containing product was obtained after solvent removal using a vacuum evaporator, with an ethyl lactate concentration of up to approximately 900 $g \cdot L^{-1}$ and PLA to ethyl lactate conversion of up to 98%. The conversion of PLA to ethyl lactate increased proportionally with increasing PLA content in the respective material**,** at the expense of additives and impurities. The lowest amount of ester product was observed for PLA-F**,** in which the natural polymer fraction (cellulose) comprised at least 50%

of the sample; this specimen also exhibited the lowest degree of overall material decomposition (Figure 1, Table 2).

The conversion of PLA to ethyl lactate (X_{PLA}) was calculated based solely on the PLA fraction in the composite materials, excluding inert fillers and non-converted components. This approach reflects the true chemical conversion of PLA, independent of the total composite mass. For the cellulose-rich PLA-F laminate, this calculation reveals a relatively high conversion of the PLA fraction despite the lower overall degradation of the composite material. However, because the exact PLA/cellulose ratio is not known, the calculated *X*(PLA) value for PLA-F should be considered approximate (Table 2).

It should be noted that the conversion values presented in Figure 2 represent the time-dependent conversion during the alcoholysis reaction, whereas the final *X*(PLA) values reported in Table 2 and Figure 1 were calculated from the ethyl lactate concentration determined after solvent removal and concentration of the product fraction.

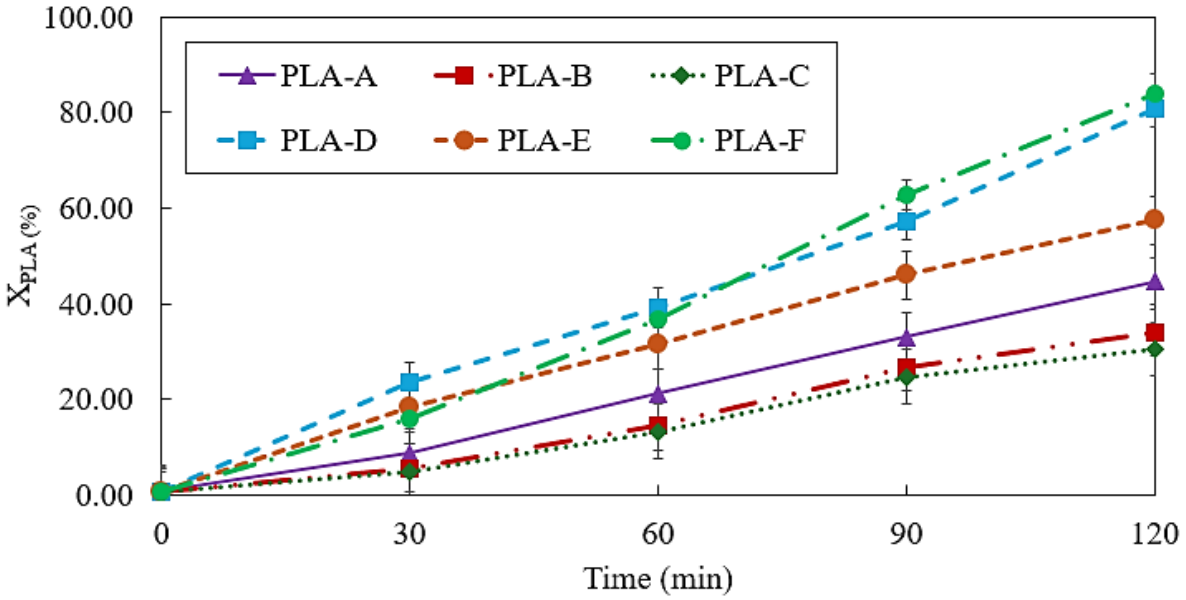
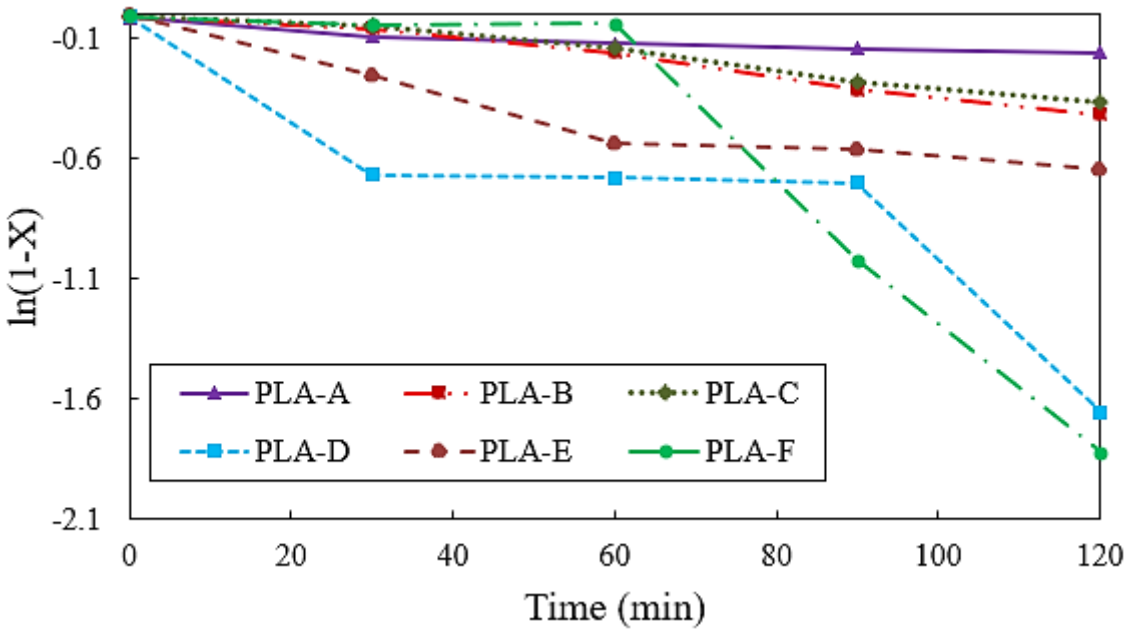


Figure 2 Effect of alcoholysis time on the conversion of PLA to ethyl lactate, calculated with respect to the PLA fraction in the composite materials, RSD: 5.1 ± 0.3% (three or more

422 measurements); PLA-D at 120 min showed a significant difference observed between
423 replicate measurements ($P < 0.05$)
424 Ethyl lactate is an established bio-based green solvent with potential for further utilization in
425 polymer processing and other solvent-based applications. Its applicability to PLA processing
426 has recently been demonstrated by (Lovecká et al., 2025), who successfully employed ethyl
427 lactate-containing green solvent systems for PLA electrospinning as an alternative to
428 conventional DMF-based systems. Moreover, alkyl lactates obtained by PLA alcoholysis can
429 potentially serve as platform chemicals for further conversion, including lactide formation,
430 providing an additional route towards closing the PLA material cycle (Upare et al., 2012).
431 Therefore, EL formation from PLA composite materials may provide opportunities for
432 subsequent valorisation; however, its practical utilization will depend on the composition and
433 purification requirements of the recovered liquid fraction.



434
435 Figure 3 Kinetic analysis of PLA conversion to ethyl lactate during alcoholysis, based on
436 pseudo-first-order behaviour
437 Solid-loading groups: 14.3 wt% – PLA-A, PLA-B
438 4.04 wt% – PLA-C, PLA-D, PLA-E, PLA-F

Characteristic reaction times for the investigated PLA composites are summarized in Table S5 (Supplementary Information). Kinetic analysis was performed assuming first- and second-order reaction models (Table S6, Supplementary Information) to compare depolymerization behaviour. Linearization using the first-order equation, $\ln(1 - X) = -kt$, gave good correlations for most samples (R^2 = 0.80–0.98). The second-order model did not improve the fit and showed lower R^2, especially for rapidly converting samples (PLA-D and PLA-F).

As shown in Figure 3, the approximately linear relationship observed for $\ln(1-X)$ versus time suggests that the depolymerization behaviour can be reasonably described by an apparent pseudo-first-order kinetic model. However, direct quantitative comparison of the apparent rate constants between the two solid-loading groups should be treated with caution, as differences in reaction concentration and mass-transfer conditions may also contribute to the observed kinetic behaviour.

Deviations from ideal linearity were observed for PLA-D and PLA-F, likely due to heterogeneous structure and changes in accessibility of reactive sites during degradation, which may be influenced by the presence and nature of fillers and additives (Quiles-Carrillo et al., 2018). These deviations suggest that additional transport or morphology-related effects may contribute to the overall degradation behaviour of these materials. In PLA-F, the high cellulose content (>50 wt%) may contribute to reduced accessibility of the PLA phase and may partially explain the lower depolymerization efficiency observed for this material. In addition to reducing the relative PLA content, the high lignocellulosic fraction may create heterogeneous interfacial regions and more tortuous transport pathways, potentially limiting penetration of the solvent and catalyst into PLA-rich domains (Xu et al., 2026). In PLA-D, the woven stack structure combined with minor fillers creates heterogeneity, causing uneven reaction rates across the material. The applied kinetic models provide apparent rate constants

rather than intrinsic kinetic parameters. These apparent rate constants reflect not only the intrinsic chemical reactivity of PLA ester bonds but also physical factors such as ethanol penetration, accessibility of the PLA phase, material morphology, and mass-transfer limitations within heterogeneous composite structures. Consequently, differences in k values should be interpreted as a combined effect of chemical and transport-related phenomena rather than as intrinsic reaction kinetics. The relatively high apparent rate constant observed for PLA-F may be associated with cellulose-rich heterogeneous structure, which can influence reactant accessibility and transport phenomena during alcoholysis.

The degradation behaviour of PLA observed in this study is consistent with trends previously reported for pure PLA (Bergerova et al., 2025), where similar patterns in thermal decomposition and product distribution were observed. Compared to previous reports (Leibfarth et al., 2012; Majgaonkar et al., 2021), the present approach achieved high depolymerization efficiency under milder reaction conditions, such a lower reaction temperature, use of non-toxic reagents, and greater initial material quantities. Nevertheless, limitations such as slower kinetics or sensitivity to feedstock purity should be addressed in future work to enhance practical applicability. Overall, the results indicate that composition and material form primarily determine depolymerization efficiency and kinetic behaviour under comparable alcoholysis conditions.

3.2 Characterization of PLA composite waste during chemical treatment

3.2.1 Determination of the molecular weights (M_w) of the polymer materials

Molecular weight (Mw) was determined for the original materials prior to alcoholysis and for the residual polymer after the reaction using gel permeation chromatography (GPC) (Table S7, Supplementary Information).

For PLA-A and PLA-D, total decomposition prevented determination of Mw values, as no residual polymer remained. The molecular weights of samples diminished in parallel with the degree of polymer decomposition (PLA-B, C, E). PLA-F initially had a molecular weight of 45 kDa, which decreased to 6 kDa after degradation, indicating extensive PLA degradation, with the residual fraction primarily consisting of cellulose and low-molecular-weight fragments (Bergerova et al., 2025; Huang and Wang, 2009; Leibfarth et al., 2012).

These results confirm that molecular weight reduction is consistent with the observed degradation trends and supports the interpretation of compositional effects on alcoholysis efficiency.

3.2.2 Thermochemical characterization of tested materials

DSC and TGA were employed to characterize the thermal behaviour of PLA materials before and after solvolysis, in order to evaluate the effects of additives on alcoholysis treatment on crystallinity and thermal stability of materials.

3.2.2.1 Characterization of the thermal behaviour of materials using DSC

DSC analysis revealed variations in melting temperatures and degrees of crystallinity among the original PLA materials, their dry matter after dissolution in chloroform, and the residues obtained after alcoholysis. The dissolution of the original materials in chloroform was performed to dissolve the PLA matrix and additives, resulting in a more homogeneous and predominantly amorphous material, and enabling a clearer interpretation of the DSC thermal transitions.

Although the differences between the original and dissolved samples in terms of melting temperatures and degrees of crystallinity were relatively small, measurable variations were

observed, as reflected by the T_m and χ_c values listed in Table S1 (Supplementary Information). The observed thermal behaviour was influenced by the presence of fillers and additives, manifested by shifts in T_g, cold crystallization, and changes in χ_c, which help rationalize differences in depolymerization performance. DSC was used mainly to rationalize differences in degradation behaviour, while detailed thermal parameters are provided in the Supplementary Information (Chapter SI 1, Figure S1–S3).

In line with these DSC observations, thermal stability was further evaluated by TGA.

3.2.2.2 Thermal stability and degradation behaviour of materials using TGA

Thermal stability and degradation behaviour of the PLA materials before and after alcoholysis were evaluated by thermogravimetric analysis (TGA), with the onset of decomposition defined as a 5% mass loss (Figures 4 and 5).

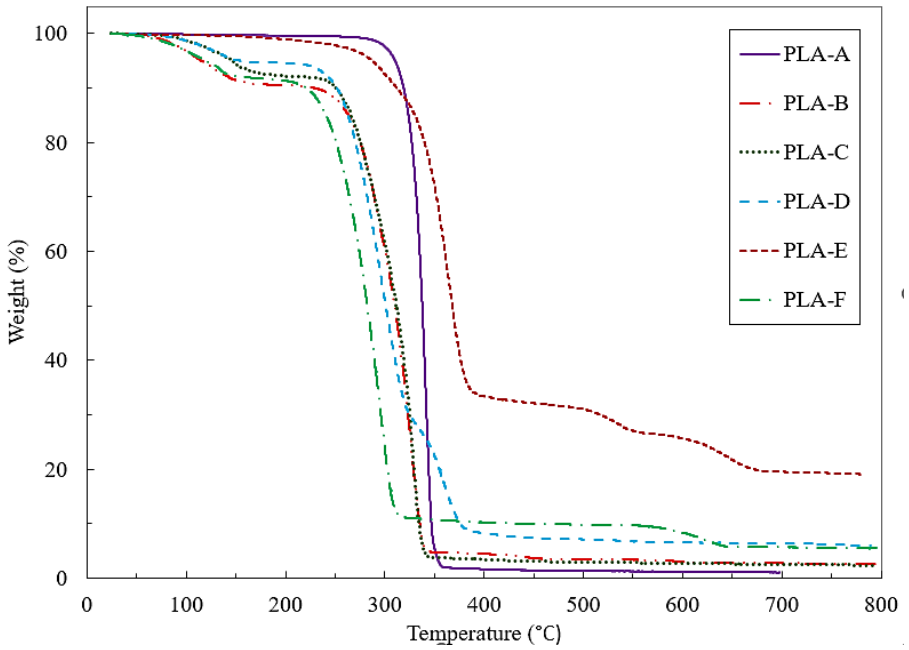


Figure 4 TGA curves of the input PLA (A-F) samples

Figure 4 shows the TGA curves of the original PLA materials (PLA-A–F). A detailed sample-specific interpretation of degradation stages and quantitative residue analysis is provided in the Supplementary Information (Section SI 2). All samples exhibited an initial mass loss below 250 °C, commonly attributed to the presence of moisture and/or low-molecular-weight components (Cuadri and Martín-Alfonso, 2018; Faba et al., 2024; Hopmann et al., 2015; Meng et al., 2012; Signori et al., 2009; Södergård and Stolt, 2002; Zou et al., 2009) . The pure PLA-A sample underwent a single-step thermal degradation process, with decomposition occurring mainly between 300-350 °C and an onset temperature of approximately 305 °C, consistent with the reported thermal behaviour of neat PLA (Azarian and Sutapun, 2022; Leibfarth et al., 2012; Liendo et al., 2022; Majgaonkar et al., 2021).

In contrast, PLA materials containing fillers and additives exhibited earlier degradation onsets and more complex, multi-step decomposition profiles. In particular, the presence of calcium carbonate ($CaCO_3$) led to a reduction in thermal stability compared to pure PLA, which has been attributed to the catalytic effect of mineral fillers on the depolymerization of PLA ester bonds (Betancourt and Cree, 2017; Pavon et al., 2022). The incorporation of plasticizers further contributed to a decrease in decomposition temperature, in agreement with literature reports on plasticized PLA systems (Betancourt and Cree, 2017; des Ligneris et al., 2020; Román-Ramírez et al., 2020). Conversely, samples containing a higher proportion of cellulose exhibited enhanced thermal stability, confirming the stabilizing effect of cellulose on polymer matrices reported previously (Kato et al., 1998).

Overall, thermal degradation of PLA occurred predominantly within the temperature range of 150–400 °C (the lower onset being associated with the presence of plasticizers and low-molecular-weight components), corresponding to chain scission degradation mechanisms (Azarian and Sutapun, 2022; Liendo et al., 2022). The observed differences among the

samples reflect variations in additive content, crystallinity, and structural characteristics of the PLA matrices.

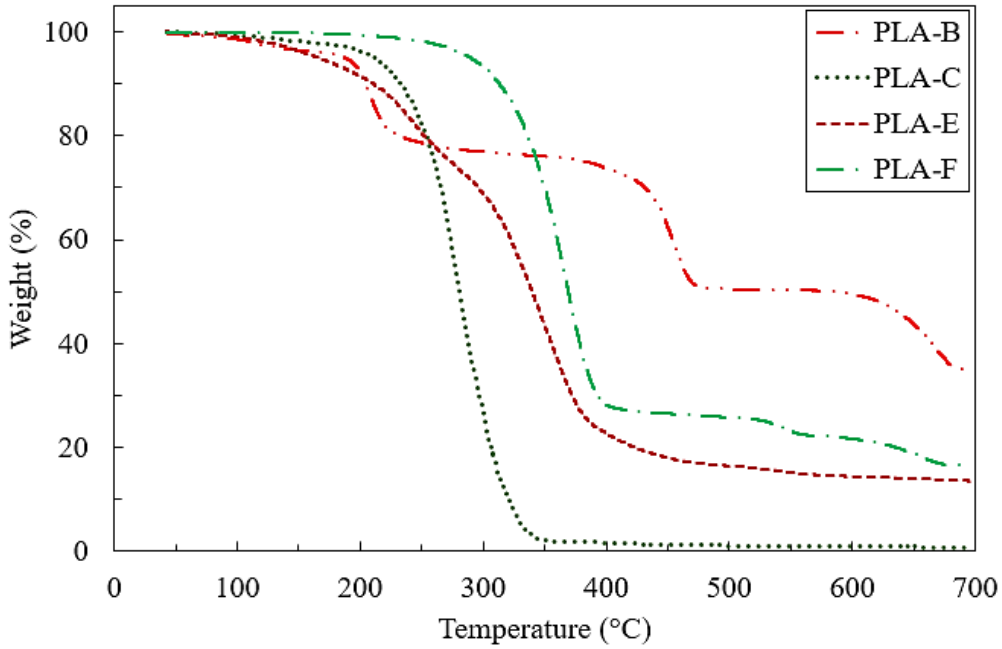


Figure 5 TGA curves of the PLA (B, C, E, F) samples after alcoholysis

Since PLA-A and PLA-D were fully decomposed during alcoholysis, they were not further evaluated by TGA. The post-alcoholysis samples generally exhibited lower decomposition onset temperatures and higher relative inorganic residue contents, reflecting the removal of the PLA matrix and the enrichment of inorganic components, particularly $CaCO_3$ (Betancourt and Cree, 2017; Pudełko et al., 2021; Siddiqui et al., 2021). A comprehensive discussion of the individual degradation steps and residual mass fractions is given in the Supplementary Information (Section SI 2). In materials with higher cellulose content, increased resistance to thermal degradation was retained even after alcoholysis, in agreement with DSC observations (Kato et al., 1998).

Taken together, TGA confirmed that the thermal stability and degradation behaviour of the investigated PLA materials were strongly influenced by the presence of fillers, plasticizers,

and secondary polymeric components. These findings are consistent with the DSC results and demonstrate the combined effect of material composition and solvolysis treatment on the thermal response of PLA. Detailed sample specific TGA interpretation and quantitative residue analysis are provided in the Supplementary Information (Chapter SI 2).

The presence of a residual solid fraction after alcoholysis is further supported by DSC and TGA analyses, which reveal thermal transitions and degradation profiles corresponding to non-PLA components. In particular, cellulose-rich samples and materials containing inorganic fillers exhibit characteristic thermal stability and residual mass, confirming that these components persist after selective depolymerization of the PLA matrix.

3.2.3 Chemical structures of tested materials

The investigated polymers were analysed by XRD and ATR-FTIR, with XRD used primarily to identify crystalline phases. The diffractograms of each PLA material are detailed in Figure 6.

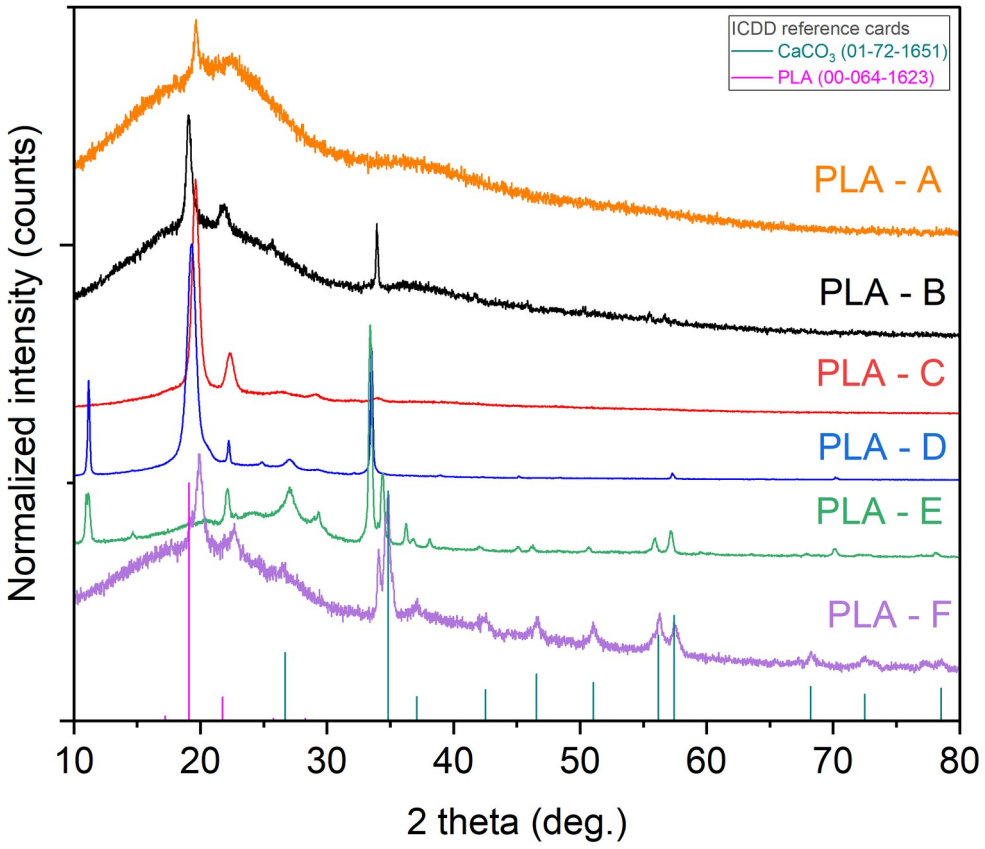


Figure 6 Powder X-ray diffractograms for the dry mass of PLA (A-F) with reference cards: ICDD PDF (00-064-1623, and 01-072-1651). Patterns are vertically offset for clarity

Figure 6 presents X-ray diffraction patterns for the PLA materials as dry mass (PLA-A-F). XRD revealed diffraction lines between 16° and 23° 2 theta, and less prominent diffractions between 26°–40°. Diffractions appearing at ~12–18° and in the range 40-70° 2 theta suggest the presence of additional phases associated with additives or secondary polymer matrices. As illustrated in Figure 6, diffraction patterns were matched to PLA ICDD PDF reference card with number 00-064-1623. The slight shifts in the PLA diffraction peaks are most likely caused by inhomogeneous morphology and differences in the macroscopic structure of the samples, which can lead to small variations in their positioning on the sample holder. Based on the diffractograms, the components could be assigned. The diffractograms indicate variations in filler content and material form among the investigated samples (granules, foils, woven stack). After dissolution of PLA (A-E) samples in chloroform and solvent evaporation,

the materials exhibited reduced crystallinity, reflecting disruption of the original polymer morphology (see the DSC results in Supplementary information, Table S1). The PLA-A pure polymer exhibited predominantly amorphous character with only weak diffraction maxima (Table S1, Figure 6). Characteristic broad reflections typical of semi-crystalline PLA were observed in the region of approximately 16-23 °. XRD analysis demonstrated the presence of additives in sample PLA-B, PLA-E compared with pure PLA-A. PLA-D displayed additional diffraction peaks at approximately 12°, 35°, 58° and 70°, indicating the presence of secondary polymeric components or additives (Table 1). PLA-E contained distinct peaks in the regions of 10°, 35°, 58° and 70°, but differed from those in the case of PLA-D due to double peaks in the area 55-58°. These differences suggest the presence of additional polymeric components in sample E (for example some cellulose), consistent with the compositional data in Table 1. Based on the XRD patterns, the PLA samples denoted as B, E, F contain an inorganic filler $CaCO_3$ (a slight peak appears at ca 34-35 °), assigned to ICDD PDF card 01-072-1651. Inorganic fillers (e.g., $CaCO_3$) were identified in PLA-C, while additional features potentially associated with carbon black were observed in PLA-B and PLA-E (Figure 6, Table 1). In PLA-F, cellulose peaks may overlap with PLA reflections in the 20–22° region, making unambiguous identification difficult. According to the literature, peaks for PLA identification are in the area at 18 – 22°, which corresponds to the XRD patterns observed for the examined materials (PLA-A-F) (Quiles-Carrillo et al., 2018).

The ATR-FTIR spectra of all PLA-based composites were recorded to verify the presence of characteristic functional groups and assess any structural modifications induced by additives. The spectra confirm the expected chemical structures, and no unexpected peaks were observed. FTIR spectra are provided in the Supplementary Information (SI 3; Figure S4–S9).

3.2.4 Elemental analysis of PLA composites

Elemental analysis was performed to determine the composition of the composites and quantify the content of inorganic fillers and additives. The results indicate good agreement with nominal formulations and confirm the successful incorporation of all components. Elemental composition of the composites is summarized in Table S4 (Supplementary information, Chapter SI 4).

Overall, the main structural and compositional characteristics of the composites confirm successful incorporation of additives and support the observed trends in alcoholysis depolymerization efficiency.

3.2.5 Limitations and Future Directions

Despite the promising results obtained in this study, several limitations must be acknowledged. The alcoholysis conditions (using acetone as the solvent, ethanol as the nucleophile, a single organic catalyst, and fixed temperature/time parameters) were not optimized for each material type, which may influence degradation efficiency across different formulations. However, the conditions were based on an optimized procedure described by Domincová Bergerová et al. (Bergerova et al., 2025), originally developed for PLA materials, where high product yield and purity were demonstrated. Moreover, only six PLA-based materials were tested. While representative of common additive types, they do not encompass the full diversity of commercially available PLA composites or post-consumer waste. The mechanistic role of individual additives on the alcoholysis process was inferred from overall trends rather than investigated directly at the molecular level. In addition, the study did not assess environmental impacts or economic aspects, which are critical for evaluating the feasibility of large-scale application. The applied alcoholysis conditions were comparatively

mild and based on the use of environmentally benign reagents relative to previously reported methods (Carné Sánchez and Collinson, 2011; Szatkowski et al., 2024) .

Solvent recovery was not quantitatively evaluated in the present study and therefore remains a limitation of the current process assessment. Preliminary experiments on TBD recovery resulted in recovery efficiencies of approximately 20–35%, while catalyst reuse was associated with reduced efficiency. These preliminary observations indicate that further optimization of catalyst recovery and reuse is required before repeated recycling cycles can be reliably implemented.

Future work should address these limitations by expanding the scope to include industrial waste streams and post-consumer PLA composites. Systematic optimization of solvolysis parameters and kinetic modelling could improve product yield and overall process efficiency. In-depth studies on additive–matrix interactions during alcoholysis including monitoring and molecular-level analysis, are needed to better understand the degradation mechanisms. Furthermore, techno-economic and life cycle assessment will be essential for validating the sustainability and scalability of this recycling method. Although preliminary recovery and reuse of the reaction components, including ethanol, acetone, and the TBD catalyst, have been investigated within our broader research, systematic optimization of their recovery was beyond the scope of the present study. Efficient solvent and catalyst recovery, including repeated reuse cycles, will require further investigation and represents an important aspect for future process scale-up and assessment of its economic and environmental performance.

4. Conclusion

The present study demonstrates that the depolymerization behaviour of commercially relevant PLA composite materials is strongly influenced by material composition and structure.

Granular and woven stack materials with high PLA content (≥90 wt%) exhibited complete or near-complete depolymerization, whereas laminated and cellulose-rich composite structures showed reduced conversion possibly associated with limited accessibility of ester bonds within the heterogeneous matrix. Although additives influence crystallinity and thermal stability, the results suggest that compositional parameters play an important role in depolymerization performance and product formation.

The highest PLA conversion to ethyl lactate (98.80%) was achieved for neat PLA-A. PLA-based materials containing relatively low amounts of commonly used inorganic fillers and modifiers, such as calcium carbonate (<1.5 wt%), carbon black, and plasticizers, also showed high conversion, indicating that these components did not substantially hinder alcoholysis under the applied conditions. In contrast, high additive contents, particularly cellulose-rich matrices (>50 wt%), were associated with lower overall depolymerization efficiency, suggesting that such compositionally complex materials may represent more challenging feedstocks for alcoholysis under the applied conditions. This effect may be related to changes in accessibility of reactive ester bonds and altered degradation kinetics associated with the cellulose-rich structure. Minor amounts (<1 wt%) of secondary polymers, such as DETPE or PBAT, showed no significant impact on the alcoholysis process. These findings indicate that process performance is governed not only by additive content but also by additive chemical nature and its influence on polymer architecture, crystallinity, and accessibility of ester bonds within heterogeneous composite matrices.

All investigated PLA-based materials underwent substantial depolymerization under the applied reaction conditions, despite pronounced structural differences confirmed by XRD and ATR-FTIR analyses. Differences in thermal degradation onset were associated with variations

in molecular weight (M_w), glass transition (T_g), melting temperature (T_m), and composite formulation, consistent with the observed degradation behaviour.

The novelty of this work lies in extending previous alcoholysis studies from virgin PLA to commercially relevant multi-component PLA composites and in evaluating the depolymerization behaviour of representative industrial materials. The results provide practical insight into how composite composition and material structure may affect depolymerization efficiency and ethyl lactate formation in commercially relevant PLA-based materials. Overall, the alcoholysis approach investigated in this study represents a promising chemical treatment strategy for PLA composite waste streams, enabling resource recovery in the form of ethyl lactate and supporting the circular management of bioplastic materials.

CRediT authorship contribution statement

Domincova Bergerova Eva: Conceptualization, data curation, investigation, methodology, project administration, validation, visualization, roles/writing - original draft; **Sedlarik Vladimir:** supervision, writing - review & editing, formal analysis, funding acquisition; **Cisar Jaroslav, Strasakova Monika, Uhercova Simona, Hanusova Dominika, Dusankova Miroslava and Skoda David:** methodology, investigation.

Declaration of competing interests

The authors declare that they have no conflict of interests.

Acknowledgements

This work was supported from the European Just Transition Fund within the Operational Programme Just Transition under the aegis of the Ministry of the Environment of the Czech Republic, project CirkArena number CZ.10.03.01/00/22_003/0000045 and the Ministry of Education Youth and Sports of the Czech Republic, Operational Programme Johannes Amos

Comenius OP JAC “Application potential development in the field of polymer materials in the context of circular economy compliance (POCEK)”, number CZ.02.01.01/00/23_021/0009004 and from the Horizon Europe programme under the project BioPackMan – Biodegradable Packaging Materials Advancing Circularity, Sustainability & Eco-Innovation (Grant Agreement No. 101178576). Authors are further grateful for co-funding from the development process of Centre of Polymer Systems, Tomas Bata University in Zlín, programme DKRVO (RP/CPS/2024-28/002) and (RP/CPS/2024-28/007) supported by the Ministry of Education Youth and Sports of the Czech Republic.

Data availability

Data will be made available on request.

Declaration of generative AI and AI-assisted technologies in the manuscript preparation process

During the preparation of this work, the authors used ChatGPT (OpenAI) to assist in the preparation of the graphical abstract and to improve the language and readability of the manuscript. After using this tool, the authors reviewed and edited the content as needed and take full responsibility for the content of the publication.

Reference

Alaerts, L., Augustinus, M., Van Acker, K., 2018. Impact of bio-based plastics on current recycling of plastics. Sustainability (Switzerland) 10. https://doi.org/10.3390/su10051487

Bagliotta, L., Cinelli, P., Coltelli, M.B., Righetti, M.C., Gazzano, M., Lazzeri, A., 2017. Effect of nucleating agents on crystallinity and properties of poly (lactic acid) (PLA). Eur. Polym. J. 93, 822–832. https://doi.org/10.1016/j.eurpolymj.2017.04.041

Carrigo, R., Bartoli, M., Malucelli, G., 2020. Poly(lactic Acid)-biochar biocomposites: Effect of processing and filler content on rheological, thermal, and mechanical properties. Polymers (Basel). 12, 1–13. https://doi.org/10.3390/POLYM12040892

Auras, R., Harte, B., Selke, S., 2004. An overview of polylactides as packaging materials. Macromol. Biosci. https://doi.org/10.1002/mabi.200400043

Azarian, M.H., Sutapun, W., 2022. Biogenic calcium carbonate derived from waste shells for advanced material applications: A review. Front. Mater. 9, 1–17. https://doi.org/10.3389/fmats.2022.1024977

Balla, E., Daniilidis, V., Karlioti, G., Kalamas, T., Stefanidou, M., Bikiaris, N.D., Vlachopoulos, A., Koumentakou, I., Bikiaris, D.N., 2021. Poly(lactic acid): A versatile biobased polymer for the future with multifunctional properties-from monomer synthesis, polymerization techniques and molecular weight increase to PLA applications. Polymers (Basel). https://doi.org/10.3390/polym13111822

Behrens, A., 2016. Time to connect the dots: What is the link between climate change policy and the circular economy? Brussels.

Bergerova, E.D., Strasakova, M., Cisar, J., Sopik, T., Dusankova, M., Vincent, I., Klaban, J., Hanusova, D., Uhercova, S., Hanykova, L., Sedlarik, V., 2025. Impact of solvolysis on the decomposition efficiency of poly(lactic acid) materials with insight into their non-uniform architecture. Int. J. Biol. Macromol. 302, 140529. https://doi.org/10.1016/j.ijbiomac.2025.140529

Betancourt, N.G., Cree, D.E., 2017. Mechanical Properties of Poly (lactic acid) Composites Reinforced with CaCO3 Eggshell Based Fillers. MRS Adv. 2, 2545–2550. https://doi.org/10.1557/adv.2017.473

Carné Sánchez, A., Collinson, S.R., 2011. The selective recycling of mixed plastic waste of polylactic acid and polyethylene terephthalate by control of process conditions. Eur. Polym. J. 47, 1970–1976. https://doi.org/10.1016/j.eurpolymj.2011.07.013

Cisar, J., Drohsler, P., Pummerova, M., Sedlarik, V., Skoda, D., 2023. Composite based on PLA with improved shape stability under high-temperature conditions. Polymer (Guildf). 276. https://doi.org/10.1016/j.polymer.2023.125943

Coman, A.E., Ionescu, G., Gîfu, I.C., Teodorescu, G.M., Magdziarz, A., Mărculescu, C., 2026. Development and characterization of PLA-based hybrid composites reinforced with chicken bone-derived fillers. J. Environ. Chem. Eng. 14. https://doi.org/10.1016/j.jece.2026.122487

Cuadri, A.A., Martín-Alfonso, J.E., 2018. Thermal, thermo-oxidative and thermomechanical degradation of PLA: A comparative study based on rheological, chemical and thermal properties. Polym. Degrad. Stab. 150, 37–45. https://doi.org/10.1016/j.polymdegradstab.2018.02.011

Cvek, M., Paul, U.C., Zia, J., Mancini, G., Sedlarik, V., Athanassiou, A., 2022. Biodegradable Films of PLA/PPC and Curcumin as Packaging Materials and Smart Indicators of Food Spoilage. ACS Appl. Mater. Interfaces 14, 14654–14667. https://doi.org/10.1021/acsami.2c02181

de Les Ligneris, E., Dumée, L.F., Kong, L., 2020. Nanofibers for heavy metal ion adsorption: Correlating surface properties to adsorption performance, and strategies for ion selectivity and recovery. Environ. Nanotechnol. Monit. Manag. 13, 100297. https://doi.org/10.1016/J.ENMM.2020.100297

Ellis, S., Buchard, A., Junkers, T., 2024. Depolymerisation of poly(lactide) under continuous flow conditions. Chem. Sci. 16, 211–217. https://doi.org/10.1039/d4sc05891g

Erwin T. H. VinkSteve Davies, 2015. Life Cycle Inventory and Impact Assessment Data for 2014 Ingeo ® Polylactide Production. Industrial Biotechnology 11, 167–180.

Erwin T.H. Vink a, Karl R. Rábago, David A. Glassner b , Patrick R. Gruber, 2003. Applications of life cycle assessment to NatureWorks™ polylactide (PLA) production. Polym. Degrad. Stab. 403419.

Gaba, S., Agüero, Á., Arrieta, M.P., Martínez, S., Romero, J., Torres, A., Galotto, M.J., 2024. Foaming of 3D-Printed PLA/CaCO3 Composites by Supercritical CO2 Process for Sustainable Food Contact Materials. Polymers (Basel). 16, 798. https://doi.org/10.3390/polym16060798

Kinnerty, J., Rowe, S., Howard, T., Connolly, S., Doran, C., Devine, D.M., Gately, N.M., Chyzna, V., Portela, A., Bezerra, G.S.N., McDonald, P., Colbert, D.M., 2023. Effect of Mechanical Recycling on the Mechanical Properties of PLA-Based Natural Fiber-Reinforced Composites. Journal of Composites Science 7, 1–17. https://doi.org/10.3390/jcs7040141

Geyer, R., Jambeck, J.R., Law, K.L., 2017. “Production , use , and fate of all plastics ever made” CA 93106; Bren School of Environmental Science and Management, University of California, Santa Barbara, Santa Barbara, USA. Sci. Adv. 3, 25–29.

Khanbarzadeh, B., Almasi, H., 2013. Biodegradable Polymers, in: Chamy, R., Rosenkranz, F. (Eds.), Biodegradation – Life of Science. IntechOpen. https://doi.org/10.5772/56230

González-López, M.E., Martín del Campo, A.S., Robledo-Ortíz, J.R., Arellano, M., Pérez-Fonseca, A.A., 2020. Accelerated weathering of poly(lactic acid) and its biocomposites: A review. Polym. Degrad. Stab. 179. https://doi.org/10.1016/j.polymdegradstab.2020.109290

Hopmann, C., Schippers, S., Höfs, C., 2015. Influence of recycling of poly(lactic acid) on packaging relevant properties. J. Appl. Polym. Sci. 132, 1–6. https://doi.org/10.1002/app.41532

Huang, N., Wang, J., 2009. A TGA-FTIR study on the effect of CaCO3 on the thermal degradation of EBA copolymer. J. Anal. Appl. Pyrolysis 84, 124–130. https://doi.org/10.1016/j.jaap.2009.01.001

Ineke Velghe, MURAKAMI, M., 1993. Melt Processing. Melt Processed High-Temperature Superconductors 21–44. https://doi.org/10.1142/9789814335898_0003

Kato, T., Suzuki, T., Amamiya, T., Irie, T., Komiyama, M., Yui, H., 1998. Effects of macromolecules on the crystallization of CaCO3 the Formation of Organic/Inorganic Composites. Supramolecular Science 5, 411–415. https://doi.org/10.1016/S0968-5677(98)00041-8

Künkel, A., Becker, J., Börger, L., Hamprecht, J., Koltzenburg, S., Loos, R., Schick, M.B., Schlegel, K., Sinkel, C., Skupin, G., Yamamoto, M., 2016. Polymers, Biodegradable, in: Ullmann’s Encyclopedia of Industrial Chemistry. Wiley-VCH Verlag GmbH & Co. KGaA, Weinheim, Germany, pp. 1–29. https://doi.org/10.1002/14356007.n21_n01.pub2

[18] Leibfarth, F.A., Moreno, N., Hawker, A.P., Shand, J.D., 2012. Transforming Polylactide into Value-Added Materials. J Polym Sci Part A: Polym Chem 50, 4814–4822. https://doi.org/10.1002/pola.26303

[21] Liendo, F., Arduino, M., Deorsola, F.A., Bensaid, S., 2022. Factors controlling and influencing polymorphism, morphology and size of calcium carbonate synthesized through the carbonation route: A review. Powder Technol. 398, 117050. https://doi.org/10.1016/j.powtec.2021.117050

[25] Liu, X., Khor, S., Petinakis, E., Yu, L., Simon, G., Dean, K., Bateman, S., 2010. Effects of hydrophilic fillers on the thermal degradation of poly(lactic acid). Thermochim. Acta 509, 147–151. https://doi.org/10.1016/J.TCA.2010.06.015

[28] Lovecká, L., Kovářová, M., Hanušová, D., Kimmer, D., Poláchová, A., Sedlařík, V., 2025. Application of green solvents as a replacement of toxic dimethylformamide in the polylactic acid electrospinning process. Sustainable Materials and Technologies 44. https://doi.org/10.1016/j.susmat.2025.e01405

[32] Majgaonkar, P., Hanich, R., Malz, F., Brüll, R., 2021. Chemical Recycling of Post-Consumer PLA Waste for Sustainable Production of Ethyl Lactate. Chemical Engineering Journal 423. https://doi.org/10.1016/j.cej.2021.129952

[35] Meng, Q., Heuzey, M.C., Carreau, P.J., 2012. Control of thermal degradation of polylactide/clay nanocomposites during melt processing by chain extension reaction. Polym. Degrad. Stab. 97, 2010–2020. https://doi.org/10.1016/j.polymdegradstab.2012.01.030

[38] Ravon, C., Aldas, M., Samper, M.D., Motoc, D.L., Ferrandiz, S., López-Martínez, J., 2022. Mechanical, Dynamic-Mechanical, Thermal and Decomposition Behavior of 3D-Printed PLA Reinforced with CaCO3 Fillers from Natural Resources. Polymers (Basel). 14. https://doi.org/10.3390/polym14132646

[42] Rudełko, A., Postawa, P., Stachowiak, T., Malińska, K., Dróżdż, D., 2021. Waste derived biochar as an alternative filler in biocomposites - Mechanical, thermal and morphological properties of biochar added biocomposites. J. Clean. Prod. 278. https://doi.org/10.1016/j.jclepro.2020.123850

[46] Quiles-Carrillo, L., Montanes, N., Garcia-Garcia, D., Carbonell-Verdu, A., Balart, R., Torres-Giner, S., 2018. Effect of different compatibilizers on injection-molded green composite pieces based on polylactide filled with almond shell flour. Compos. B Eng. 147, 76–85. https://doi.org/10.1016/j.compositesb.2018.04.017

[50] Rathin Datta, M.H., 2006. Lactic acid: recent advances in products, processes and technologies . Journal of Chemical technology and Biotechnology.

[52] Román-Ramírez, L.A., McKeown, P., Jones, M.D., Wood, J., 2020. Kinetics of Methyl Lactate Formation from the Transesterification of Polylactic Acid Catalyzed by Zn(II) Complexes. ACS Omega 5, 5556–5564. https://doi.org/10.1021/acsomega.0c00291

[55] Samir, A., Ashour, F.H., Hakim, A.A.A., Bassyouni, M., 2022. Recent advances in biodegradable polymers for sustainable applications. Npj Mater. Degrad. 6. https://doi.org/10.1038/s41529-022-00277-7

Schneider, M., Fritzsche, N., Puciul-Malinowska, A., Balić, A., Mostafa, A., Bald, I., Zapotoczny, S., Taubert, A., 2020. Surface etching of 3D printed poly(lactic acid) with NaOH: A systematic approach. Polymers (Basel). 12. https://doi.org/10.3390/POLYM12081711

Shorey, R., Mekonnen, T.H., 2024. Oleic acid decorated kraft lignin as a hydrophobic and functional filler of cellulose acetate films. Int. J. Biol. Macromol. 268, 131672. https://doi.org/10.1016/j.ijbiomac.2024.131672

Siddiqui, M.N., Redhwi, H.H., Al-Arfaj, A.A., Achilias, Dimitris S, Siddiqui, M.N.;, Redhwi, H.H.;, Al-Arfaj, A.A.;, Achilias, D S, 2021. Chemical Recycling of PET in the Presence of the Bio-Based Polymers, PLA, PHB and PEF: A Review. Sustainability 2021, Vol. 13, Page 10528 13, 10528. https://doi.org/10.3390/SU131910528

Signori, F., Coltelli, M.B., Bronco, S., 2009. Thermal degradation of poly(lactic acid) (PLA) and poly(butylene adipate-co-terephthalate) (PBAT) and their blends upon melt processing. Polym. Degrad. Stab. 94, 74–82. https://doi.org/10.1016/j.polymdegradstab.2008.10.004

Södergård, A., Stolt, M., 2002. Properties of lactic acid based polymers and their correlation with composition. Prog. Polym. Sci. 27, 1123–1163. https://doi.org/10.1016/S0079-6700(02)00012-6

Spinelli, G., Lamberti, P., Tucci, V., Kotsilkova, R., Tabakova, S., Ivanova, R., Angelova, P., Angelov, V., Ivanov, E., Maio, R. Di, Silvestre, C., Meisak, D., Paddubskaya, A., Kuzhir, P., 2018. Morphological, rheological and electromagnetic properties of nanocarbon/poly(lactic) acid for 3D printing: Solution blending vs. melt mixing. Materials 11. https://doi.org/10.3390/ma11112256

Szatkowski, P., Gralewski, J., Suchorowiec, K., Kosowska, K., Mielan, B., Kisilewicz, M., 2024. Aging Process of Biocomposites with the PLA Matrix Modified with Different Types of Cellulose. Materials 17, 1–18. https://doi.org/10.3390/ma17010022

Tadi, S.P., Mamilla, R.S., 2025. Fabrication of SS 316L particle-infilled PLA composite filaments from cast-off bi-material extrudates for 3D printing applications. Waste Management 193, 386–397. https://doi.org/10.1016/j.wasman.2024.12.021

Thakur, S., Chaudhary, J., Sharma, B., Verma, A., Tamulevicius, S., Thakur, V.K., 2018. Sustainability of bioplastics: Opportunities and challenges. Curr. Opin. Green Sustain. Chem. 13, 68–75. https://doi.org/10.1016/j.cogsc.2018.04.013

Thumsorn, S., Prasong, W., Kurose, T., Ishigami, A., Kobayashi, Y., Ito, H., 2022. Rheological Behavior and Dynamic Mechanical Properties for Interpretation of Layer Adhesion in FDM 3D Printing. Polymers (Basel). 14, 1–22. https://doi.org/10.3390/polym14132721

Tonini, D., Garcia-Gutierrez, P., Nessi, S., 2021. Environmental effects of plastic waste recycling. https://doi.org/10.2760/955772

Tsou, C.-H., Luo, H., Qu, C.-L., Potiyaraj, P., Preuksarattanawut, C., Wu, C.-S., Du, J.-H., Feng, S., Ge, F.-F., 2025. High-performance conductive nanocomposites of modified poly(lactic acid) and nanocarbon black: Enhanced mechanical properties, chemically proven 3D network structure, and antibacterial features for 3D printing. International Journal of Biological Macromolecules 322, 146683. https://doi.org/10.1016/j.ijbiomac.2025.146683

Shpare, P.P., Hwang, Y.K., Chang, J.S., Hwang, D.W., 2012. Synthesis of lactide from alkyl lactate via a prepolymer route. Ind. Eng. Chem. Res. 51, 4837–4842. https://doi.org/10.1021/ie202714n

Velghe, I., Buffel, B., Vandeginste, V., Thielemans, W., Desplentere, F., 2023. Review on the Degradation of Poly(lactic acid) during Melt Processing. Polymers (Basel). 15, 2047. https://doi.org/10.3390/polym15092047

Xia, Y., Qian, S., Zhang, X., Zhang, Z., Zhu, C., 2024. Biochar as an efficient reinforcing agent for poly(lactic acid)/poly(ε-caprolactone) biodegradable composites with high robustness and thermo-resistance. Ind. Crops Prod. 219, 119049. https://doi.org/10.1016/j.indcrop.2024.119049

Xu, N., Meng, L., Ge, F.-F., Lan, L., Du, J., Suen, M.-C., Chao, F., Huang, J., Tsou, C.-H., 2026. Reactive interfacial design enables oxygen–moisture transport regulation in PLA/cotton-stalk films for food preservation. Future Foods, 101176. https://doi.org/10.1016/j.fufo.2026.101176

Yadav, P., Farnood, R., Kumar, V., 2021. HMO-incorporated electrospun nanofiber recyclable membranes: Characterization and adsorptive performance for Pb(II) and As(V). J. Environ. Chem. Eng. 9, 106507. https://doi.org/10.1016/J.JECE.2021.106507

Zdanowicz, M., Mizielińska, M., Kowalczyk, A., 2024. Cast Extruded Films Based on Polyhydroxyalkanoate/Poly(lactic acid) Blend with Herbal Extracts Hybridized with Zinc Oxide. Polymers (Basel). 16. https://doi.org/10.3390/polym16141954

Zou, H., Yi, C., Wang, L., Liu, H., Xu, W., 2009. Thermal degradation of poly(lactic acid) measured by thermogravimetry coupled to Fourier transform infrared spectroscopy. J. Therm. Anal. Calorim. 97, 929–935. https://doi.org/10.1007/s10973-009-0121-5